Wilde, A., Simpson, L. and Hanna, S. 2002. Preliminary study of Tertiary hydrothermal alteration and platinum deposition in the Oman ophiolite. In: Jessell, M. W. 2002. General Contributions: 2002. Journal of the Virtual Explorer, 6, 7-13.

Preliminary study of Tertiary hydrothermal alteration and platinum deposition in the Oman ophiolite

A. WILDE[1], L. SIMPSON[3,4] AND S. HANNA[2]

*[1] pmd*CRC, School of Geosciences, Monash University, Melbourne, Clayton, Australia*
[2]Dept Earth Sciences, Sultan Qaboos University, Al Khodh, Oman
[3]Post Graduate Institute for Sedimentology, University of Reading, Reading, UK
[4]Now at LGC Ltd, Middlesex, UK

Abstract: We present the preliminary results of an investigation into Tertiary hydrothermal alteration of ultramafic rocks from the Semail ophiolite, Oman. We infer a Tertiary regional thermal event manifested in basaltic and basanitic dyke intrusion, extensional faulting and fluid flow. New data include field and mineralogical observations, geochemical analyses and geochemical models of alteration processes. Two types of hydrothermal alteration are documented. Carbonate-altered serpentinite is mineralogically and chemically similar to travertine that is abundant in northern Oman. The second alteration type is silica-iron oxide also known locally as "listwaenite". Both rocktypes contain anomalous but sub-economic levels of Ni and Pt, but are depleted in Cu.

Geochemical modelling has shown that ionic strength and cation contents of potential hydrothermal fluids are of less significance than oxidation state and to a lesser extent pH in mobilizing Pt from potential source rocks. Ppm levels of Pt are predicted in oxidized waters that have interacted with serpentinite, gabbro, pyritic gabbro and chromitite containing Pt metal and PtS. The rocks with highest Pt abundance (pyritic gabbro and chromitite) are not necessarily the best source rocks given that they have higher concentrations of reductant minerals. Modelling suggests that Pt release may occur in a rapid "spike" as Pt-undersaturated oxidized fluid overcomes the ability of the rock to buffer oxygen fugacity to low levels.

Prediction of economic Pt deposits requires knowledge of many variables including fluid composition, total fluid flux, flow path (i.e. rock types traversed, mainly influencing oxidation state and pH), porosity (fracture density?) and time. Understanding the hydrodynamic regime in the area is therefore critical to the prediction of ore deposits.

Introduction

The Semail ophiolite of Oman is perhaps the most intensely studied ophiolite in the world and the presence of unusual silica, iron oxide/hydroxide and carbonate hydrothermal alteration within it has long been known (Glennie et al., 1974; Stanger, 1985; Villey et al., 1986). There has been only one substantial study of this alteration (Stanger, 1985) despite the fact that in other ophiolite bodies (e.g. Morocco, Saudi Arabia) similar alteration is associated with potentially economic gold concentrations (Buisson & LeBlanc, 1985 & 1987). In this paper, we present new field observations, new mineralogical and geochemical data and geochemical models of water-serpentinite interaction. We present a preliminary hypothesis for the formation of this hydrothermal alteration and sub-economic platinum mineralization, involving high heat flow associated with post-obduction Tertiary faulting and magmatism and circulation of oxidised groundwaters similar to those present today. Relatively Pt and Pd depleted chromite pods are proposed as a possible source of these elements.

Previous Work

Glennie et al. (1974) first mapped the silicified ("listwaenite") portion of the Semail ophiolite of Oman, as the Amqat lithostratigraphic unit. Stanger (1985) noted that the Amqat unit is within the basal serpentinite, sometimes being part of a basal thrust. He inferred that silicification was spatially and temporally associated with Palaeogene fault movement. Stangers' work also suggested that the silica and iron oxides replaced serpentinised ultramafic as evidenced by the presence of (presumably residual) chromite and similar amounts of Al, Fe and Cr in serpentinite and silicified serpentinite.

Elsewhere, hydrothermally altered ophiolite (listwaenite) of Saudi Arabia, hosts ancient gold workings at the margin of serpentinised ultramafic rock masses. Hydrothermal alteration phases include talc, dolomite, magnesite, magnesian chlorite and fuchsite, while chromite is a relict, metastable phase inherited from the precursor rock (Buisson & LeBlanc, 1987). Economic gold (> 1 ppm) occurs in pyrite- and gersdorffite-rich zones and in late quartz veins, and has been observed at the margins of pyrite crystals (Buisson & LeBlanc, 1987).

Another example of precious metal associated with altered ophiolite is the Bou Azzer ophiolite in Morocco (Buisson & LeBlanc, 1985 & 1987). Small cobalt orebodies (now mined out) consisted of arsenide minerals (e.g. skutterudite) in a calcite-dolomite gangue with hematite, magnetite and quartz. About 5 tonnes of by-product gold was recovered. Elevated gold (1 – 10 ppm) occurred in rocks containing high levels of pyrite and cobalt arsenide or late pyrite and arsenopyrite-bearing quartz veins (Buisson & LeBlanc, 1985 & 1987). Gold-

rich rocks also contain high levels of Sb, Bi and Ag. The contact between ore and serpentinite was marked by a distinct talc-serpentine-carbonate zone (listwaenite) and Mg-chlorite and serpentine become more abundant with proximity to unaltered serpentinite, suggesting hydrothermal zonation.

Buisson & LeBlanc (1987) have argued that the gold was deposited from modified CO_2-rich seawater that circulated through the ophiolite during serpentinisation. They cite fluid inclusion evidence for temperatures of 150 to 250ºC. Gold was inferred to have been introduced as a sulphide or arsenide complex and precipitated due to pH change and/or change in oxidation state that resulted from interaction of hydrothermal fluid and carbonate rocks. Gold is inferred to have been derived from magnetite contained within the serpentinite.

This model contrasts with Stanger's (1985) proposed mechanism for the formation of the Amqat "listwaenite" and associated carbonate-rich rocks. He proposed an early serpentinization driven by seawater ingress into the ophiolite. The seawater was regarded as a source of arsenic. Formation of the Amqat "listwaenite" was however ascribed to circulation of slightly acidic and CO_2-rich groundwater at less than 50ºC.

Hopkinson (2001) provided an unusual explanation for the "listewaenite" involving salt diapirism through the ophiolite. The evidence for diapirism is, however, limited to the presence of rare salt-rich rocks in a fault zone at Qantab. A plausible alternative explanation is that the salt is derived from localized evaporation of contemporary groundwaters.

Geological Framework

Four Main Tectonostratigraphic Units

The geology of the study area is shown as figure 1, which is based on the mapping of Villey et al. (1986), as is the account of the regional geology given below. Four major tectono-stratigraphic units can be differentiated. The oldest rocks in the area, referred to herein as basement, are autochthonous Ordovician to Cretaceous carbonate and clastic sedimentary rocks, summarized in Table 1. Overall the rocks are red, yellow or mauve in colour. Pseudomorphs after gypsum have been noted, but appear to be uncommon. The Saiq Formation is conspicuously darker, and yields H_2S when struck with a hammer. Basaltic and andesitic volcanic rocks form a small part of the overall basement sequence. Pyroxene phenocrysts are preserved but the ground mass is commonly altered to an assemblage of epidote, chlorite and Ti-oxide of uncertain age.

Overlying the basement rocks are autochthonous rocks of the Permian Al Jil Formation, part of the Hawasina Nappes. These include alkalic basaltic to andesitic lavas, shale, conglomerate, limestone radiolarian chert and sandstone. Primary magmatic minerals include plagioclase, clinopyroxene and various opaque minerals.

Formation	*Thickness*	*Age*	*Facies*	*Lithologies*	*Comments*
MUTI	>250m	**Cretaceous**	Basin fill mega-sequence?	Sandstone & conglomerate, limestone, chert, volcanic rocks. Poor age control.	Many have red, mauve or yellow colour suggesting a relatively oxidised sequence.
				UNCONFORMITY	
KAHMAH	0 - 200m	**Late Jurassic - Cretaceous**	Variable: infra-littoral platform, sub-tidal to bathyal	Limestone locally oolitic, micritic limestone, conglomerate	Basal micritic limestone is partially silicified. Yellows, reds and mauves predominate suggesting a relatively oxidised sequence.
				UNCONFORMITY	
SAHTAN	100m	**Jurassic**	Lagoonal continental to supra-tidal (fluviatile to submarine deltaic)	Sandstone, black dolomite, siltstone. Upper massive limestone. Discontinuous conglomerate at base.	Top is a "hardground" defined by iron concentrations and secondary breccia. Probably related to silicification in overlying unit.
				UNCONFORMITY	
MAHIL	500m	**Early-Middle Triassic**	Intertidal on an "internal platform"	Grey & yellow dolomite, black limestone. Locally oolitic. "Syn-sedimentary" breccia common. Minor siltstone, sandstone & conglomerate.	Gypsum pseudomorphs have been identified. Distinctly paler than underlying unit. Overall sequence is probably relatively oxidised.
SAIQ	350 - 400m	**Permian**	Middle to proximal subtidal platform. Intertidal influence at top.	Black limestone (including coralline limestone) & dolomite "intraformational breccia". Minor conglomerate, siltstone & volcanic rocks (pyroxene-phyric basalt and andesite).	Mafic rocks have altered groundmass with epidote, chlorite & Ti oxide. Overall seuqnece appears to be reduced, although there are red and yellow-coloured rocks at base.
				UNCONFORMITY	
AMDEH	3.4 km	**Ordovician**	Variety of marginal marine facies	Sandstone (grey-green), siltstone, conglomerate & shale	Appears to be reduced (dominance of green or grey colours, only minor purple)

Table 1. Stratigraphy and lithologies of the pre-obduction autochthonous basement (compiled from descriptions in Villey et al., 1986).

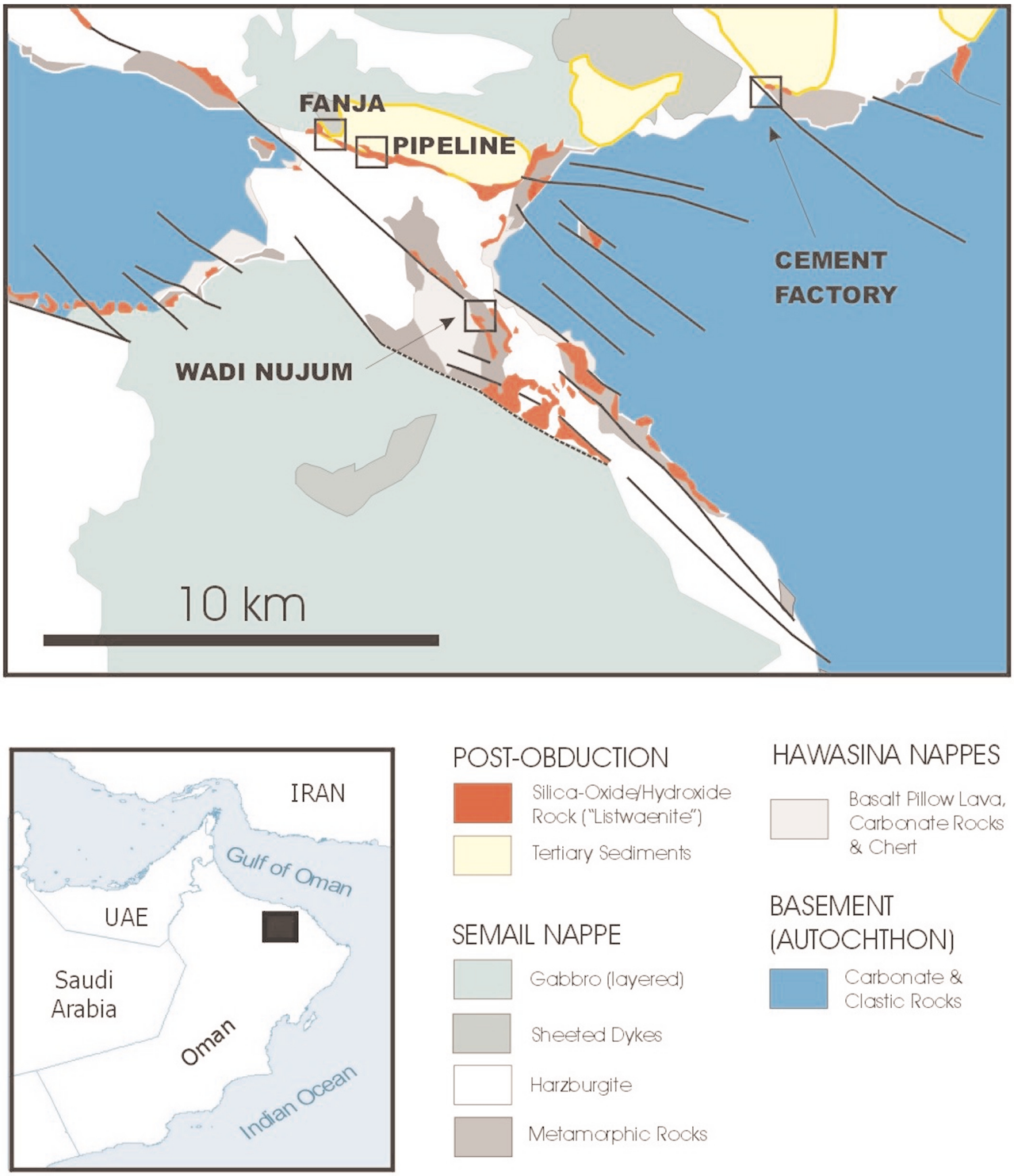

Figure 1. Geology of the Fanjah area, showing the distribution of "listwaenite" simplified after Villey et al. (1986). Quaternary deposits related mainly to wadis are not shown.

Magmatic plagioclase has been replaced by albite and carbonate and chlorite are common secondary phases. The chemical composition of the lavas suggests formation in a rift environment (Cotton et al., 2001).

The next major tectono-stratigraphic unit is the Semail nappe consisting of ophiolitic harzburgite, separated by a discontinuous dunite layer from overlying layered gabbro and a sheeted dyke unit of dolerite dykes with chilled margins. These rocks were tectonically emplaced over the basement during obduction in the Cretaceous (e.g. Hanna, 1992). Superimposition of the ophiolite sequence on underlying sediments created quartzite, garnetiferous muscovite schist, chlorite schist and amphibolite collectively known as the metamorphic sole.

About 90% of the "mantle" sequence has undergone serpentinisation of intensity varying between 55 and 85% by volume (Stanger, 1985). Veins of carbonate (mainly magnesite) are almost ubiquitous (Stanger, 1984). A range of Ni minerals has been described including acicular niccolite, annabergite, maucherite, Ni-nontronite and Ni-

montmorillonite (Haynes, 2001; Stanger, 1985; Hopkinson, 2002). Another alteration type is rodingite, found in faults and joints, consisting of hydrogrossular, prehnite and zoisite.

Overlying gabbro also displays evidence for post-intrusion hydrothermal alteration, namely the presence of tremolite-actinolite, epidote, chlorite, sphene, prehnite, talc and magnetite and locally sulphide minerals (e.g. Nehlig & Juteau, 1988). The age (or ages) of this widespread and locally intense alteration, however, remains uncertain.

Post-obduction cover rocks vary in age from Late Cretaceous to Quaternary and consist of conglomerate, limestone and sandstone unconformably overlying all older units. They were deposited in environments that range from marginal marine to inner shelf (e.g. Racey, 1994). The Tertiary rocks are unmetamorphosed, but in the vicinity of the cement factory (Fig. 1) show varying degrees of silicification, and iron metasomatism and up to 100 ppb gold has been recorded (Haynes, 2001). Locally, harzburgite faulted against the Tertiary rocks has been altered to an assemblage of Ni-montmorillonite and halloysite (Haynes, 2001).

Tertiary Extension & Inversion

Tertiary extension in northern Oman commenced just after obduction of the ophiolite and persisted until at least until deposition of the Eocene Rusayl formation (Fournier et al., 2001). The main axis of extension was NNE-SSW to NE-SW and produced numerous NW trending structures (e.g. Fig. 1; Fournier et al., 2001). Neogene compression resulted in inversion of these structures (Fournier et al., 2001).

Evidence for elevated heat flow during the early Tertiary includes the presence of minor mafic dykes that were intruded into Tertiary sediments near the cement factory at between 36 and 40 million years (Fig. 1; Al Harthy et al., 1990). This magmatic episode has also been recognised in the Batain region of NE Oman, some 250 km distant from the area of interest (Worthing and Wilde, 2002) and appears, therefore, to be of considerable extent. Spore coloration and AOM reflectance measurements on shales and coaly shales from the Rusayl Formation (outcropping about 20 km from the study area) show that maximum temperatures at the base of the Tertiary were of the order of 65ºC (Goodall et al., 2001a,b). Vitrinite reflectance data from the Abat Trough about 200 km SE of the study area also indicate unusually elevated temperatures during the Tertiary (Abdulrahman Al Harthy, unpub. data) and support the idea that this event was of regional rather than local extent.

The area of interest was partially emergent during the Tertiary (generating laterites) with adjacent mangrove tidal swamps and other warm-water shallow marine environments (El Beialy, 1998; Racey, 1994). During the Eocene, there is some evidence for hypersaline conditions in coastal lagoons (Keen & Racey, 1991). These observations are of some significance to the discussion of potential ore-forming fluids (see below).

Field & Mineralogical Observations

We recognise two main facies of hydrothermal alteration: Ca-Fe-Mg carbonate (CFM) and silica-iron hydroxide (SIH), both developed extensively (although not exclusively) in serpentinised ultramafic rocks. Figure 1 shows SIH hydrothermal alteration as mapped by Villey et al. (1986) and described as “listwaenite”. The major occurrences are clustered within an area approximately 15 by 10 km (Fig. 1) and tend to be controlled by NW-SE (post-obduction) faults and/or the base of the ophiolite sequence. The latter has been interpreted to reflect the presence of thrust fault permeability (Stanger, 1985). Some of the largest occurrences of altered rocks are along the Paleogene Fanjah fault (Hanna & Rodgers, 1996 & 2001). This is a normal fault that dips to the north with at least 6 km of normal slip and transects early thrust faults (Hanna & Rodgers, 1996 & 2001).

The distinctive SIH alteration forms linear peaks, as the rock is more resistant to erosion than adjacent carbonated serpentinite and Tertiary sediments (Fig. 2a). These peaks are incised by recent wadis and overlain by Quaternary wadi sediments. Pervasive silicification and iron metasomatism has also been noted in Tertiary limestone excavations at the cement factory (Fig. 1; Haynes, 2001). These observations strongly support a Tertiary age for the alteration event.

Individual SIH bodies are vertical or sub-vertical, typically about 10m thick, but locally up to 50m thick and associated with a reticulate stockwork of milky white quartz veins (Fig. 2b-d). Vein thickness varies from a few millimetres to several centimeters. Pervasive silicification extends outwards from the veins (interpreted as the result of fluid moving outwards from the vein conduit) and grades gradually into the carbonate-dominant alteration facies. Pervasive silicification overprints the carbonated ultramafic rocks. It is not clear, however, whether this overprinting is due to an age difference between the two alteration types or due to variation in fluid chemistry with distance from the main conduit or conduits. Rare pseudomorphs after pyrite were noted at several locations (comprising less than 1% by volume of the rock) and rosettes of gypsum were observed on some fracture surfaces. The latter are probably related to evaporation of contemporary groundwaters.

Quartz veins in SIH show a variety of textures. In some cases, where there is a high density of veins the rock is a tectonic breccia (Fig. 2b). Angular fragments can be fitted back together suggestive of high fluid pressures. Veins commonly exhibit crustiform layering, with individual bands defined by coxcomb-textured quartz. There are often central cavities in which nodular aggregates of quartz (and in some instances chalcedony) complete the paragenetic sequence. The veins show no textural evidence of boiling. For example, lattice-textured quartz after carbonate has not been observed, nor development of adularia that is typical of epithermal precious metal deposits formed as a result of boiling. Massive hematite is spatially associated with SIH at the Fanja roadcut

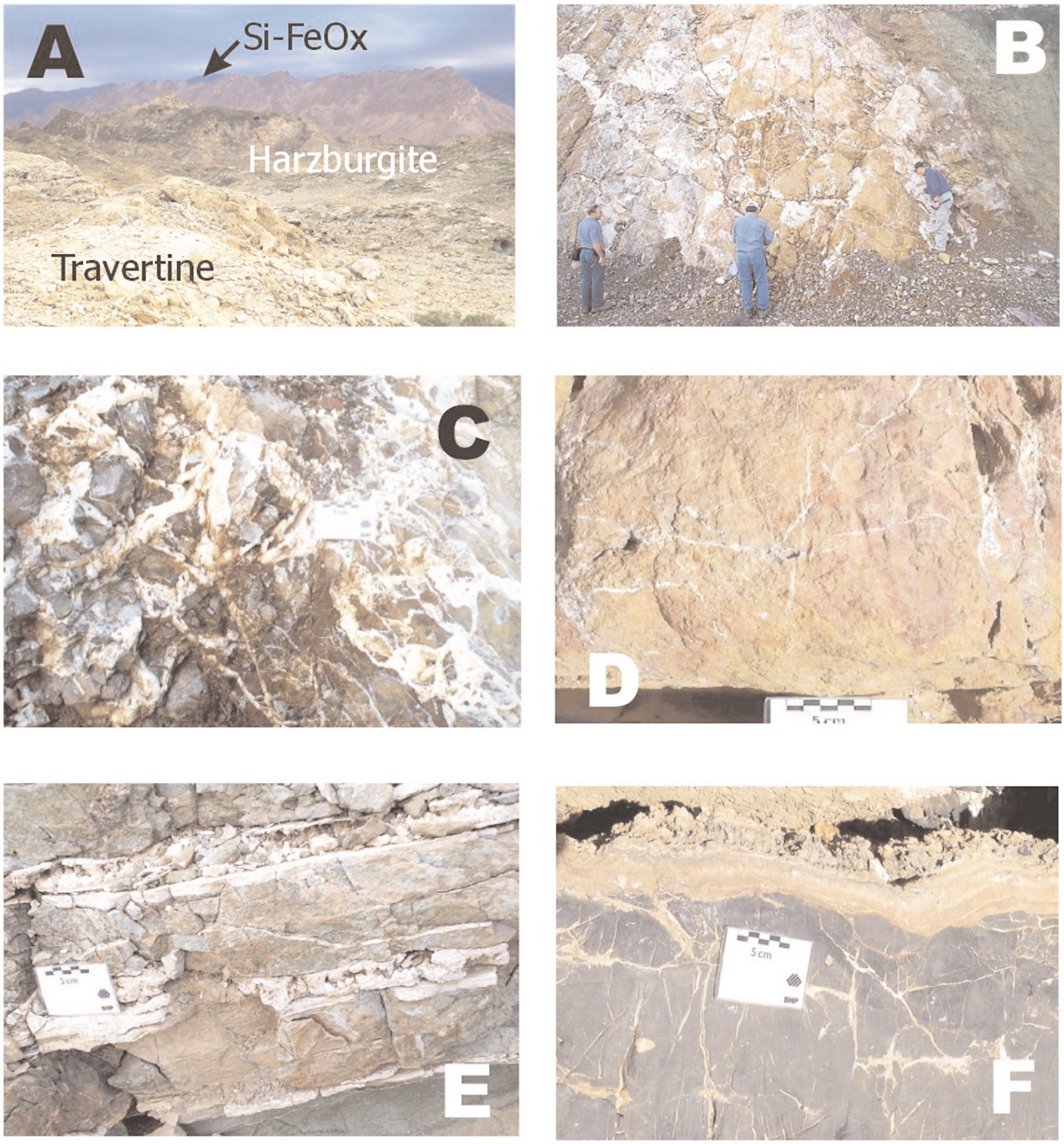

Figure 2. Photographs showing various manifestations of hydrothermal alteration. A: Ridge of silica-iron hydroxide (SIH) alteration in background with low rounded mound of pale-coloured travertine in foreground. B: One of the best exposed examples of hydrothermal alteration – Fanja roadcut. The photograph shows reticulate (stockwork) quartz veining in tan-coloured silicified host-rock. C: Close up of the above showing breccia texture, possibly indicative of high fluid pressures and hydraulic fracturing. D: Fine quartz veinlets at the "pipeline" occurrence. E: Travertine veins in serpentinised harzburgite. F: Travertine veins and coating on dolomite.

occurrence (Fig. 1) where it occupies a steeply dipping fault.

Petrographic study reveals textures that are very similar to those of the CFM rocks (Fig. 3b). The serpentinite minerals have been almost completely replaced by cryptocrystalline quartz (confirmed by XRD measurements) and hematite and/or goethite. Nevertheless the original serpentinite mesh textures are clearly visible (Fig. 3b). The CFM alteration facies is defined by pervasive replacement of serpentinite by very fine-grained carbonate (Fig. 3a). It is best developed between SIH and serpentinite in the area of interest, but we cannot be sure that such alteration is restricted to the periphery of SIH zones. CFM alteration ranges from low volumes of carbonate veinlets that mimic antigorite veinlets to massive replacement. X-ray diffraction study has demonstrated the presence of ankerite, dolomite and calcite. Phases presumably inherited from the serpentinite

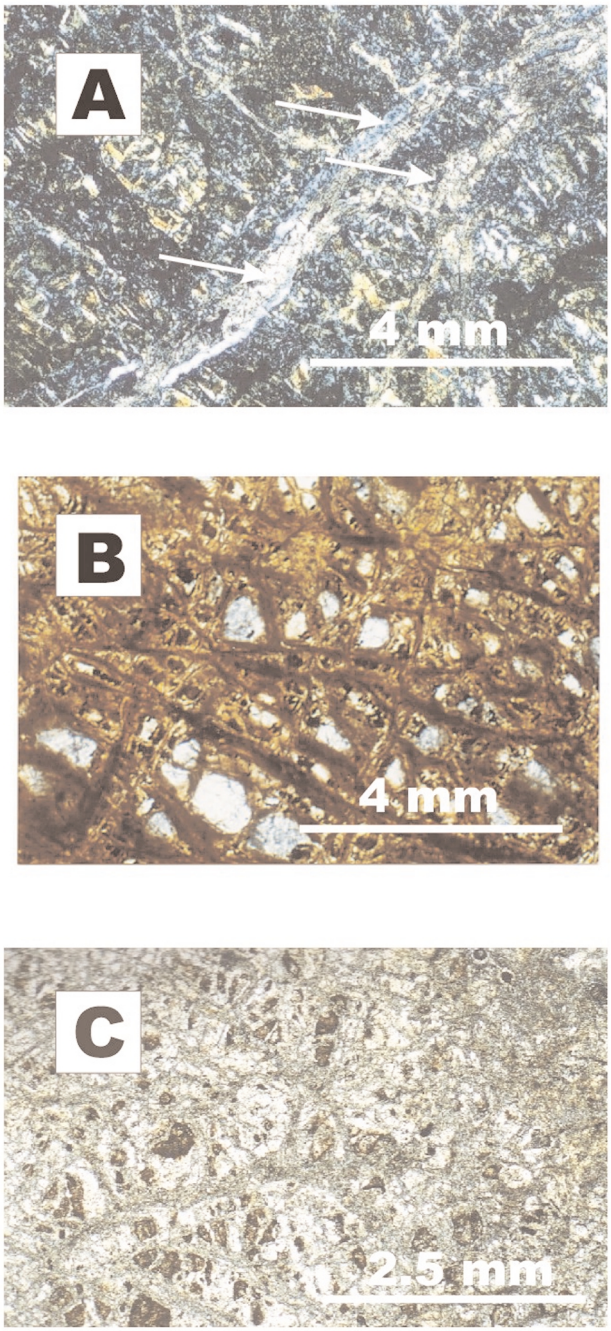

Figure 3. Photomicrographs. A: Partially carbonated serpentinite. Sample FQ4550. Crossed polars. Calcite veinlets (arrowed) exploit pre-existing serpentinite veinlets. B: SIH "Listwaenite". Sample FQ4549. Plane-polarised light. C: Travertine. Sample FQ4593. Plane-polarised light. Note evidence of serpentinite replacement.

include lizardite, antigorite and chrysotile, together with chromite and magnetite, a probable relict of the serpentinisation process.

Several samples of travertine were studied because these also represent carbonate-altered serpentinite (Fig. 3c) although there are equally obvious examples where carbonate has precipitated as a surface or joint-related coating (Fig. 2e, f). The replacive textures are remarkably similar to those of CFM-altered serpentinite adjacent to SIH.

Geochemical Analysis

Methods

Precious and base metal concentrations were determined in 16 samples of CFM and SIH alteration types using a Perkin Elmer ELAN 6000 inductively coupled plasma mass spectrometer (ICP-MS) at Reading University, UK. Samples were crushed, ground to < 30_m in an agate ball mill and homogenized. Then, 0.5g was digested on a hotplate in open Teflon vessels with hydrofluoric (HF) and perchloric ($HClO_4$) acids to ensure total digest. A 1:10 dilution was made to ensure that the samples satisfied ICP-MS instrumental limits on total dissolved solids and acidity, and 10 ppb Re and 10 ppb Ge internal standard was added. All final concentrations were mass corrected. Oxide interferences (from ZrO on Ag, YO and Pd, HfO on Pt, and TaO on Au) were corrected mathematically using correction factors derived from earlier quantification of oxide interferences relative to CeO/Ce ratios (Table 2). In addition, fifty-one new major and minor element analyses were conducted using Phillips XRF equipment at Sultan Qaboos University, Oman and standard analytical methodology. Summary results are presented in Tables 3-5.

Results & Interpretation

The carbonated serpentinite is chemically distinct from unaltered serpentinite. Significant relative enrichment in Ca and depletion in Si reflects abundance of Ca-Mg carbonate. SIH altered serpentinite consists mainly of Si (80%). Small amounts of Fe, Ca and Mg reflect the presence of small amounts of iron hydroxide and carbonate minerals. Both types of altered serpentinite contain significantly more Ni but less Cu & Zn than unaltered serpentinite. Indeed Cu, Pb and Zn are generally present at very low levels in the altered serpentinites, although there is one small occurrence at Wadi Nujum (Fig. 1). Arsenic values remain low, typically less than 20 ppm.

In order to estimate mass/volume changes attending hydrothermal alteration, geochemical analyses were plotted on isocon diagrams (Fig. 4; Grant, 1986). We first considered the possibility that carbonate-altered serpentinite represents a variant of carbonatite. Comparison with carbonatites of northern Oman (Ziegler et al, 1991; Table) reveal significant chemical differences. Higher SiO_2 and MgO in carbonate-altered serpentinite reflects lesser calcite relative to the carbonatite. The carbonatite also contains significantly higher Sr, Ba and Zn. Reference to Fig. 4 shows that most elements in carbonate-altered serpentinite fit approximately to an isocon suggesting significant mass gain during alteration (over 100%). Ca and Ni are somewhat enriched relative to the unaltered serpentinite and Cu is depleted. Thus the frequent occurrence of traces of Ni minerals in the serpentinite is interpreted as the result of hydrothermal addition, rather than relative enrichment due to volume loss. Figure 4 shows that a similar isocon can be produced

Analyte	Mass	Correction Factors	Detection Limits (ppb)
Zn	63.929	-0.035 x 60Ni	0.49
As	74.922	-3.127 x (77ArCl-(0.815 x 82Se))	0.15
Ru	101.904	-0.046 x 105Pd	0.02
Pd	104.905	-0.098 x 111Cd – 0.01515 x 90Zr	0.01
Sn	119.902	-0.013 x 125Te	0.02
Hf	179.947	-0.0001 x 181Ta – 0.005 x 182W	0.04
Pt	194.965	-0.01143 x 179Hf	0.002
Au	196.967	-0.01049 x 181Ta	0.09

Table 2. Correction factors for oxide interferences. Detection limits for ICP-MS analyses, calculated by replicate (n5) analysis of the relative standard deviation of the blank solution, since blank concentrations are the main limiting factor in the detection limits achievable in PGE analysis (Frimpong et al., 1995).

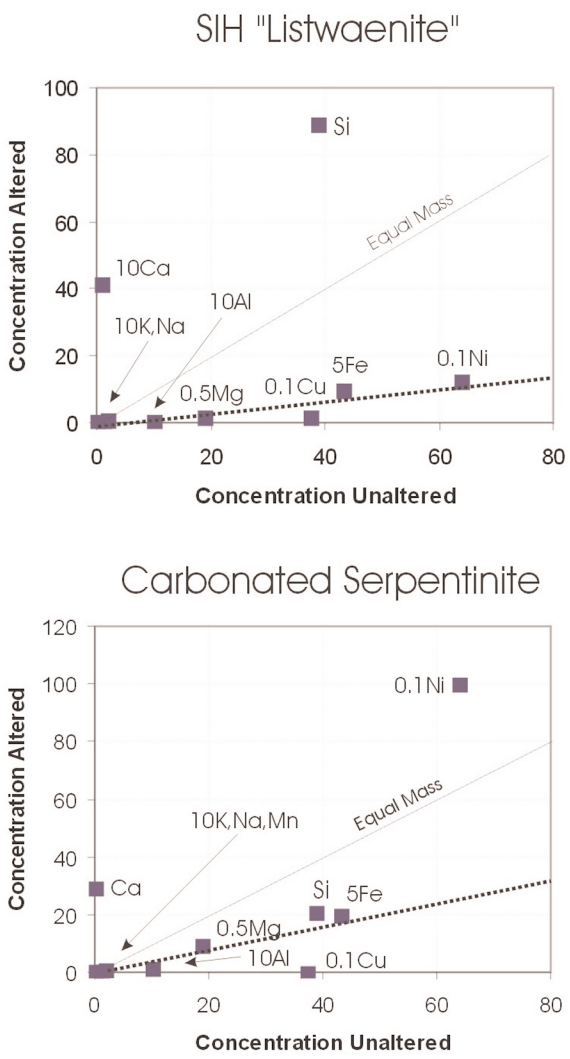

Figure 4. Isocon diagrams (Grant, 1986) showing relative mass changes between unaltered and altered serpentinites.

for the SIH alteration, but the slope suggests greater mass gain (mainly of Si and Ca), consistent with abundant evidence of veining. Cu depletion is also a feature of alteration in the SIH serpentinites, although Ni appears to have been immobile during SIH alteration.

Table 5 lists some analyses of several samples of travertine collected from inactive spring sites (mounds). Travertine samples are poorer in the mafic indicators Ni and Cr and richer in Sr due to greater abundance of carbonate minerals. The Ni and Cr contents of the rocks are, however, considerably higher than might be expected from a pure carbonate precipitate. It is not surprising that petrographic study reveals that some of the travertine samples preserve textural evidence of replacement of serpentinite (Fig. 3). Sulphur is also conspicuously enriched, and is probably present as a sulphate mineral or minerals rather than a sulphide. The striking similarity between CFM alteration and contemporary travertine, both mineralogically and chemically, suggests a similar process of formation.

Table 5 shows that many of the studied samples are notably enriched in Pt. Values of between 200 to 400 ppb Pt are common. While these values are an order of magnitude lower than those required for economic extraction, they suggest an unusual hydrothermal concentration process. No Pt-bearing minerals have been detected to date.

Geochemical Modelling

Software & Computational Methods

A series of chemical models were performed using the software Geochemist's Workbench (Bethke, 1996, herein referred to as GWB) to investigate whether various waters could mobilize ore-forming amounts of Pt from various possible source rocks and what were the likely depositional mechanisms. These took two forms: titration and flush models (see Bethke, 1996). The former simulates the addition of increments of rock to a fixed mass of hydrothermal solution, the reverse of what geologists usually consider to be the case in fluid-rock interaction. We need to differentiate between integrated fluid:rock representing the total fluid flux over the life of the hydrothermal system and the instantaneous fluid:rock representing the volume ratio of fluid to rock at a moment in time, controlled by porosity. Titration models can

Wt% Rocktype	# Samples	SiO_2	TiO_2	Al_2O_3	Fe_2O_3	FeO	MnO	MgO	CaO	Na_2O	K_2O	P_2O_5	Cl	Comments
SERPENTINITE	2	38.70	0.00	1.05	nd	8.63	0.12	37.54	0.08	0.18	0.00	nd	nd	Stanger, 1985.
CARBONATITE	22	11.85	1.01	2.14	2.14	8.50	0.61	6.01	34.11	0.56	0.13	5.87	nd	Ziegler et al., 1991
CARBONATED SERPENTINITE	3	21.79	0.00	0.35	nd	4.92	0.08	25.49	21.50	0.08	0.03	nd	0.07	This study. All Fe as FeO
LISTWAENITE (SIH)	10	79.05	0.01	0.13	nd	4.26	0.05	3.57	4.59	4.32	0.02	nd	0.17	This study. All Fe as FeO
nd = not determined														

Table 3. Summary major element data for various lithologies from the basal part of the Oman ophiolite. From various sources and new analyses from this study, using XRF.

ppm	#	As	Cu	Pb	Zn	Ni	Co	Cr	Ba	Cl	Sr	S	V	Comments
SERPENTINITE	2	60	373	-	255	638	-	-	-	-	-	-	-	Le Blanc et al., 1991
CARBONATITE	22	3	20	17.0	340	108	49	108.0	1677	-	3222	-	69	Ziegler et al., 1991
CARBONATED SERPENTINITE	16	3	21	1.0	54	2309	61	1939	58	726	137	629	48	This study
LISTWAENITE (SIH)	31	12	15	2.0	46	1202	54	1038	69	1660	97	499	72	This study
TRAVERTINE	4	1	6	-	84	341	37	203	65	562	383	2804	46	This study

Table 4. Compilation of summary minor/trace element data for various lithologies from the basal part of the Oman ophiolite and new ICP-MS analyses of this study. Analytical results in parts per million (ppb) unless stated.

		ppm		ppb							
Rocktype	#	Cu	Ni	Au	Pd	Pt	Rh	Os	Ir	Ru	Source
UNALTERED ROCKS											
Sulphidic gabbro	1	3310	2050	8	148	24	0.4		0.2	3.1	*Lorand & Juteau, 2000 (see also LaChize et al., 1991)*
Sulphide separate from gabbro	1			69	662	119	52	0.80	2.0	6.8	*Lorand & Juteau, 2000 (see also LaChize et al., 1991)*
Chromitite	30	32	700		11	17	11		49.4	184.3	*Page et al., 1982*
Gabbro	25	306	217	2	4	3	1	0.14	0.4	5.2	*Lorand & Juteau, 2000*
Serpentinite	1	373	638		16	10					*LeBlanc et al., 1991*
"White" serpentinite	1			200	3000	1300					*LeBlanc et al., 1991*
ALTERED ROCKS											
Carbonated serpentinite	(20) 5	(18)	(2124)	5	24	446	4		3.1	0.6	*This study*
Listwaenite (SIH)	(31) 11	(14)	(1202)	7	26	448	4		1.5	4.8	*This study*

Table 5. Summary precious metal data for various lithologies from the basal part of the Oman ophiolite. Analytical results in parts per billion (ppb) except Ni and Cu which are reported in parts per million (ppm).

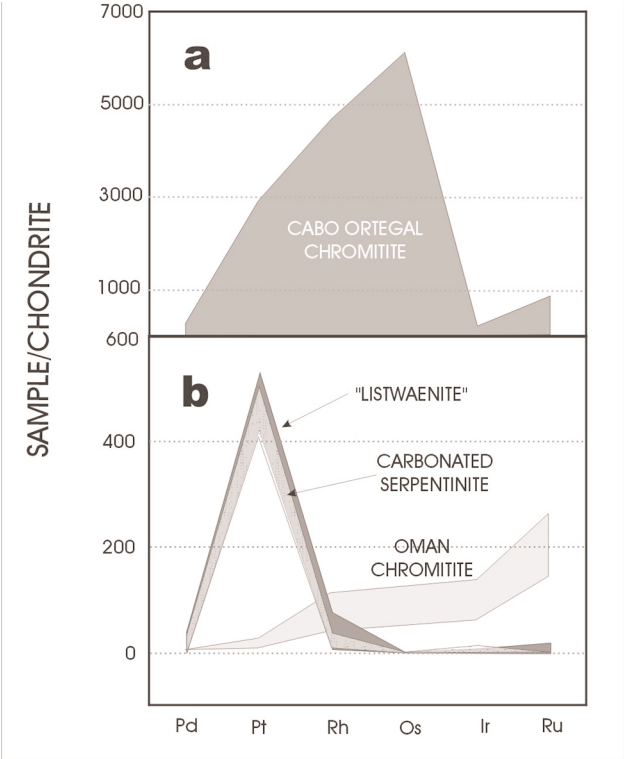

Figure 5. Spider diagram showing the ranges of platinum-group metals in various lithologies, including chromite from Oman and Spain (Moreno et al., 2001).

	METEORIC WATER		SEAWATER	BITTERN
	Gabbros & basalts	Hyperalkaine (Ultramafics)		
pH	8.3	11.6	8.8	10.8
I	0.02	0.01	0.58	2.54
Solution density (g/cm^3)	1.01	1.01	1.02	1.08
Dissolved Solids (mg/kg)	23,657	22,957	45,630	164,484
mg/kg				
Ca^{2+}	123	59	411	1211
Mg^{2+}	57	0.3	1290	0.1
Na^{+}	291	217	10760	53050
K^{+}	3	11	399	4746
HCO_3^{-}	268	2	142	0.7
SO_4^{2-}	420	15	2710	96
Cl^{-}	349	302	19350	88070
SiO_2	nd	4	6	0.2

Table 6. Representative hydrothermal fluid compositions (from Stanger, 1984; Stanger & Neal, 1984).

involve extremely high fluid:rock ratios that represent unrealistically high instantaneous fluid:rock unless reaction is taking place in a fluid-filled cavity. Nevertheless, such models can provide important insights into what are the most important variables.

We also carried "flush" experiments in which a mass of rock is specified (and which changes due to additions or reductions due to fluid-rock reaction) and a specified mass of hydrothermal fluid is passed through the rock in a series of increments displacing an equivalent volume of existing "pore" fluid (Bethke, 1996). We can approximate porosity by specifying the volume of rock in the initial stage of the calculation and by choosing an appropriate mass (volume) of fluid. Porosity is therefore independent of the total amount of fluid flushed through the model rock (see Bethke, 1996, for further discussion). Thus, this type of calculation approximates more closely the processes of nature.

The current version of GWB uses a database that is in part derived from the various SUPCRT compilations (see Bethke, 1996 and references therein). Thermodynamic properties for various aqueous Pt species are derived from the compilation of Sassani and Shock (1998).

Choice of Hydrothermal Fluid Composition

A reconnaissance for fluid inclusions as part of this study has failed to provide suitable material for thermometric analysis. Thus, we have little direct information regarding the temperature and composition of waters involved in hydrothermal alteration. Palaeoclimatic data cited earlier suggest that at least three distinct fluid types may have participated in the Tertiary alteration event or events. Meteoric water was available during times of emergence, but marine water and evaporated seawater are alternatives. Other fluid types such as magmatic, metamorphic (due to devolatisation reactions) and basinal brines are unlikely given the geological setting. As an approximation of meteoric water we have used the composition of present day groundwaters. Stanger (1984) has documented two main groundwater compositions: slightly alkaline water found in gabbros and basalts of the ophiolite ("crustal groundwater") and hyperalkaline water found in serpentinised ultramafic rocks. Thus, calculations were performed with four fluid compositions (Table 6).

We surmise that maximum temperatures in the listwaenite bodies during the Tertiary were less than 65ºC based on the studies of the Rusayl Formation (see above). Stanger (1985) estimated that the formation of niccolite and maucherite in the altered ophiolite occurred at a temperature of 40 – 45ºC based on Ni:As ratio. This conclusion was based, however, on extrapolation of experimental data from 200ºC and furthermore, there is textural evidence of disequilibrium between the two minerals (Stanger, 1985). Present day hyperalkaline water is inferred to have circulated to depths of 700m based on anomalously hot temperatures at springs, which are as much as 8ºC hotter than ambient, and a geothermal gradient of 20ºC/km (Stanger, 1984).

A significant uncertainty is the oxidation state of the waters, which was arbitrarily assumed to be in equilibrium with atmospheric oxygen. Whether Pt is carried as a chloride complex or as an hydroxyl complex, solubility is strongly dependent on oxidation state.

Possible Sources of Pt and Model Rock Compositions

Table 5 lists a compilation of published and our new PGE analyses of rocks from Oman. Enriched Pt rocks include chromite pods of the "mantle sequence" harzburgites, magmatic sulphides from ophiolite gabbro and serpentinite. Chromite pods in the Semail ophiolite

	ROCKTYPE			
%mass	**Serpentinite**	**Chromitite**	**Gabbro**	**Pyritic Gabbro**
Antigorite	49	25		
Chrysotile	49	25		
Magnetite	2		5	4
Diopside			39	36
Anorthite			32	29
Albite			24	21
Chromite		50		
Pyrite				10
Platinum	0.01	0.1	0.01	0.01

Table 7. Modal composition of rocks used in geochemical modelling

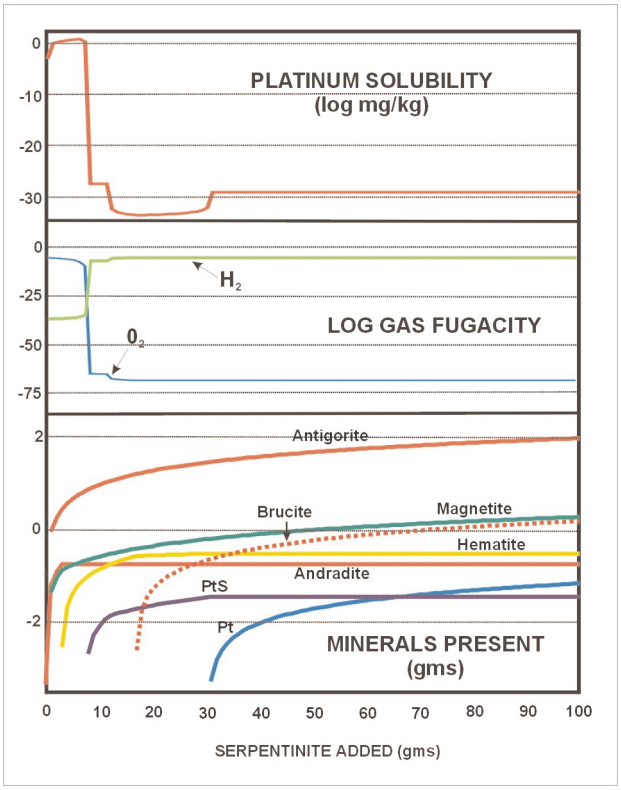

Figure 6. Titration of model serpentinite into modern-day hyperalkaline groundwater . This model illustrates the dependence of Pt solubility on oxidation state. Compare this model to the more realistic flush model in Fig. 7.

are hosted by the basal harzburgite and commonly contain elevated Ir, Ru and Rh but generally low Pt and Pd (Page et al., 1982). Magmatic silicates in these pods are often partially to completely replaced by serpentine minerals, indicating passage of late hydrothermal (metamorphic) fluid. In other environments, chromites can be considerably enriched in Pt and Pd relative to Ir, Ru and Rh (e.g. Spain, Moreno et al., 2001; Fig. 5). It is possible, therefore, that the PGE patterns of Oman chromites reported by Page et al., (1982) represent Pt and Pd depletion by hydrothermal fluids.

Another possible source lies in magmatic sulphide concentrations in the gabbroic portion of the ophiolite (e.g. Lorand & Juteau, 2000). Whole-rock PGE concentrations of economic levels have not been located so far, but as much as 120 ppb Pt has been detected in a sulphide separate (Table 5). These PGE-enriched sulphides are somewhat rare, certainly in comparison to chromitite pods. Extreme Pt-enrichment has been recorded in a single sample of pale-coloured serpentinite reported by LeBlanc et al. (1991; Table 5). There has not been a systematic attempt to find similar Pt-rich rocks in Oman and whether this represents a possible source rock or indeed an economic host in its own right remains to be seen.

Thus our models used serpentinite, chromitite, gabbro and sulphidic gabbro (Table 7) in an attempt to understand what makes a good Pt source rock in this environment. Pt minerals used in the calculations were metallic Pt and PtS (which is stable depends mainly on the sulphur concentrations adopted and oxidation state).

Results

One hundred grams of the model serpentinite was titrated into the four water compositions tabulated in Table 6. Despite the large differences in ionic strength and cation ratios the resultant mineralogies are remarkably similar. For example, all “altered” serpentinites are dominated by antigorite, brucite and hematite. Minor (< 1% by mass) phases include andradite and calcite (meteoric waters), phlogopite and calcite (bittern) and dolomite (seawater). Platinum solubility is extremely high (over 1 mg/kg) in the early part of the reaction paths as oxygen fugacity remains high (Fig. 6). Platinum solubility is accounted for by a hydroxyl complex equivalent to $Pt(OH)_{2(aq)}$. As more of the rock is titrated into the fluid it rapidly reduces the fluid and the platinum concentration drops off dramatically. The reaction is:

$$Pt(OH)_{2(aq)} \rightarrow 2H_2O + 0.5O_2 + Pt \quad (1)$$

Thus, oxidation state and high pH seem to be more important factors in mobilizing platinum than the considerable variation in water composition.

We carried out a number of flush models at 35ºC both at high porosity and at low porosity, using the four water compositions described above. For high porosity models, the rock mass was set at 100kg and the notional pore space

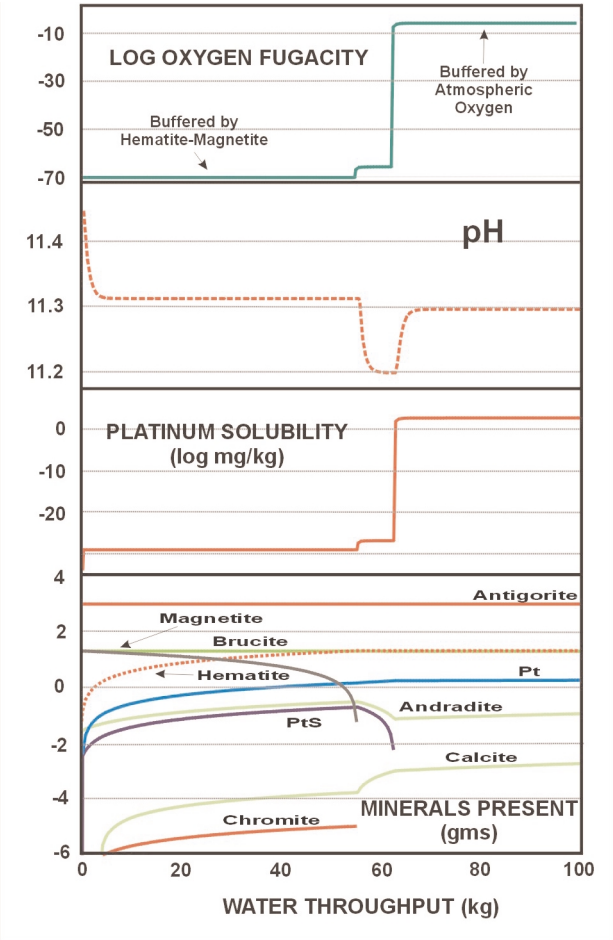

Figure 7. Flush model of modern-day hyperalkaline groundwater (with oxidation state initially buffered by atmospheric oxygen) through model serpentinite. The key insight from this model is that the ability to leach Pt is governed by the presence of magnetite. The oxidation state of the fluid is buffered at a level much lower than that required to promote solubility of native Pt as Pt hydroxide complexes, until all magnetite is destroyed, after about 50 kg of fluid has passed through the rock (i.e. integrated fluid:rock mass ratio of over 20:1).

was occupied by 1.2 kg of fluid. Then 100 kg of fluid was flushed through displacing an equivalent mass of fluid from the previous step. For the low porosity step a rock mass of 10 kg was used and all other parameters were the same. Thus, the integrated fluid:rock was between one and two orders of magnitude higher (10:1 by mass) than the instantaneous fluid:rock (1:10 or 1:100).

Flushing the four potential source rocks (Table 7) with the four oxidized waters (Table 6) resulted in a "spike" in fluid Pt concentration (> 1 mg/kg) in most cases, because in the early stages of reaction progress oxidation state is buffered by various minerals (namely magnetite, chromite, pyrite) and solubility remains low. As the oxidized fluid consumes the reductant minerals, oxidation state approaches the original atmospheric condition and Pt solubility increases dramatically. The fluid remains undersaturated in Pt thus dissolving all Pt present in the rock, although Pt concentrations vary slightly between models due to variations in pH. The drop off in fluid Pt content is due to replacement by the incoming oxidized but Pt-poor fluid. In the case of the chromitite, however, reaction lead to a much larger drop in pH to 7.5 and lower oxidation state. This in turn meant that the fluid was undersaturated in Pt and consequently Pt in the fluid was buffered by the presence of Pt metal (at about 0.45 mg/kg). Increasing the amount of Pt in the rock means that not all Pt is dissolved instantaneously and the Pt concentration of the fluid is relatively constant as demonstrated by Fig. 7.

We conclude that providing the incoming fluid is very oxidized Pt will be easily removed from serpentinite and gabbro, regardless of fluid composition. It would take a vastly greater amount of fluid to leach Pt from the chromitite, however, because of the greater abundance of reductant minerals and pH buffering to near neutral. We have taken no account of kinetic factors of course. The rapid Pt "spike" predicted in serpentinite and gabbro assumes rapid dissolution of Pt with respect to flow rate and a network of fractures such that a transient fluid is able to come into contact with the Pt (and assuming diffusion is neglible).

Depositional mechanisms were investigated by titrating various substances into a platiniferous water equilibrated with chromitite at the higher porosity. Adding CO_2 gas resulted in the generation of a magnesite and Cr oxide rock. No Pt was precipitated, as oxidation state remained high. Adding an equal mass of CH_4 resulted in complete extraction of Pt from the fluid and generation of magnesite, brucite, carbon, magnesiochromite and minor dolomite and antigorite. The Pt grade of this rock is predicted to be 450 ppb. The mechanism of precipitation of Pt is clearly reduction, with oxygen fugacity falling over 60 orders of magnitude during the reaction path. Titrating 10 grams of serpentinite resulted in extraction of some Pt resulting in a grade of about 50 ppb, with an antigorite-hematite assemblage. About 10 ppm Cr was added to the rock.

Removing Cr from the incoming fluid has a significant effect on the resulting rock. The stable assemblage is quartz, hematite and Pt phases similar to the observed SIH alteration with talc and pyrite formed at later stages of fluid rock reaction (Fig 8). Extremely large fluid:rock ratios are required for the formation of the SIH assemblage (5 gms rock:1 kg fluid). This is consistent with the abundant evidence of fracturing in the SIH serpentinite and evidence of mass gain from the bulk chemical analyses.

Discussion

The modelling demonstrates the ease with which Pt can be removed from potential source rocks within the Semail ophiolite by a variety of oxidized natural waters. Rocks richest in Pt however, aren't necessarily the best source rocks as elevated Pt is usually accompanied by higher masses of reductant minerals. The reducing capacity as well as platinum concentration of the source rock also has a crucial effect on the Pt composition of successive batches of outgoing fluid. Most rocks studied here would produce a spike of Pt-enriched water, while the chromitite

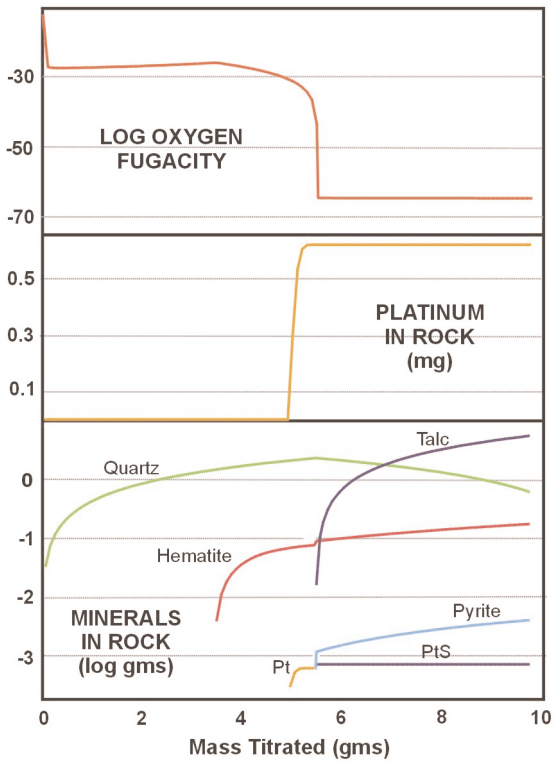

Figure 8. Titration of 10 grams of unaltered serpentinite into 1 kg of "platiniferous" fluid (interacted with platiniferous serpentinite). The SIH "listwaenite" assemblage is reproduced at relatively high fluid:rock ratios.

would generate a fluid with lower but constant Pt content. Porosity has been identified as a key variable, controlling the amount of fluid throughput required to effect Pt removal. Redox buffering of the fluid is more effective at lower porosity requiring greater fluid throughput in order to extract Pt. In reality, porosity probably equates to fracture density and morphology.

An important question is whether the processes described above could give rise to an economic deposit of Pt. Grades similar to those in nature have been simulated by interacting Pt-rich fluid from various ophiolite lithologies with "fresh" serpentinite. Such models simulate movement of oxidized fluid through a section of the serpentinised basal ophiolite (e.g. along a fault) and its subsequent interaction with unaltered serpentinite, perhaps as the result of a second faulting event and consequent fluid flow. Platinum grade in the altered rock is a function of the Pt content of the incoming fluid and the bulk composition of the depositional site. The former is shown to be dependent on time (fluid flow history), flow path (i.e. rock types traversed, mainly influencing oxidation state and pH), porosity (fracture density?) and mass of fluid. Understanding the hydrodynamic regime in the area is therefore critical to the prediction of ore deposits.

Conclusions

Two types of Tertiary hydrothermal alteration have been described in serpentinite of the Semail ophiolite, Oman. Alteration involved massive addition of carbonate or silicification along faults that developed during extension and after obduction of the Semail ophiolite, a period of regional high heat flow reflected in intrusion of basanite and basaltic magma of continental affinity. Both alteration types are somewhat enriched in Pt. Likely hydrothermal fluids include meteoric, seawater and bittern, due to periodic emergence of the Tertiary landmass from an environment of mangrove swamp and saline coastal flats.

Geochemical modelling has provided some insights into hydrothermal processes. Important constraints on the Pt content of hydrothermal waters within the Semail ophiolite are fluid flux (integrated fluid:rock), porosity (probably density of fracturing), oxidation state, pH and the availability of discrete Pt minerals. The ionic strength and cation ratios of the fluid (i.e. derivation) appear to be of much lesser importance. Knowledge of the hydrodynamic regime and better understanding of fluid chemistry at the time of alteration would permit prediction of ore-grade Pt occurrences.

References

Al Harthy, M. S., Coleman, R. G., Hughes-Clark, M. W., Hanna, S. S., 1990, Tertiary basaltic intrusions in the Cedntral Oman Mountains: in Peters, T., Nicolas, A., Coleman, R. J., (eds) "Ophiolite Genesis and the Evolution of the Oceanic Lithosphere", pp. 675-682.

Bethke, C. M., 1996, Geochemical Reaction Modelling: Oxford Uni. Press, 397 pp.

Buisson, G. & LeBlanc M., 1985, Gold in Carbonatized Ultramafic Rocks from Ophiolite Complexes: Econ. Geol., V80, pp. 2028-2029.

Buisson G. & LeBlanc M., 1987, Gold in Mantle Peridotites from Upper Proterozoic Ophiolites in Arabia, Mali & Morocco: Econ. Geol., V82, pp. 2091-2097

Cotton J., Bechenec, F., Caroff, M. and Marcoux, J., 2001, Magmatic Evolution of the Tethyan Permo-Triassic Oman Margin: Abstracts International Conference on the Geology of Oman, p.60

El Beialy, S. Y., 1998, Stratigraphic and Palaeoenvironmental Significance of Eocene Palynomorphs from the Rusayl Shale Formation, Al Khawd, Northern Oman: Rev. Palaeobotany & Palynology, V.102, pp. 249-258.

Fournier, M., Lepvrier, C., Jolivet, L., 2001, Post-Obduction Extension in Northern Oman: Abstracts International Conference on the Geology of Oman, p.33.

Frimpong, A, Fryer, B.J, Longerich, H.P, Chen, Z. and Jackson, S.E., 1995, Recovery of precious metals using nickel sulphide fire assay collection: Problems at nanogram per gm concentrations: Analyst. V120, pp. 1675 – 1680

Goodall, J.G.S., & Racey, A., 2001a, Palynology of the Early-Middle Eocene Rusayl Formation, Northern Oman: Abstracts International Conference on the Geology of Oman, p.37.

Goodall, J.G.S., Al Sayigh, A.R.S. & Racey, A., 2001b, Sequence Stratigraphy and Petroleum potential of the Early-Middle Eocene Rusayl Formation, Northern Oman: Abstracts of the International Conference on the Geology of Oman, p. 38.

Grant J.A., 1986, The Isocon Diagram – A Simple Solution to

Gresens' Equation for Metasomatic Alteration: Econ. Geol., V81, pp. 1976-1982.

Hanna, S. S., 1992, The Geology, Tectonics and Structures of the Oman Mountains from Pre-Permian to Recent: Abstracts of the 29th International Geological Congress, pp. 431.

Hanna, S. S. & Rodgers, D., 2001, Post-Orogenic Extension in Northern Oman: The Fanjah Range-Front Fault: Abstracts of the International Conference on the Geology of Oman, p. 40.

Hanna, S. S. & Rodgers, D., 1996, The Range-Front Fault of Northern Oman And Its Effect On The Hydrocarbon Potential Of The Gulf of Oman Basin: GeoArabia V1/1, p. 145.

Haynes, L., 2001, Mineralization Styles in Northern Oman Unrelated to the Ophiolite: Field Guide to Excursion A08, International Conference on the Geology of Oman, MCI, Oman, 56 pp.

Hopkinson, L., 2001, A Novel Mineralisation Style Associated with Evaporite Diapirism Through Ophiolite Assemblages: Muscat, Sultanate of Oman: Abstracts 25th AGM Mineral Deposits Studies Group, p. 36.

Keen M.C., Racey, A., 1991, Lower Eocene Ostracods from the Rusayl Formation of Oman: J. Micropal., V10/2, pp.227-233

Lachize, M., Lorand, J.P., Juteau, T., 1991, Cu-Ni-PGE Magmatic Sulfide Ores and Their Host Layered Gabbros in the Haymiliyah Fossil Magma Chamber (Haylayn Block, Semail Ophiolite, Oman): in Peters, T., Nicolas, A., and Coleman R. G., (eds), Ophiolite Genesis and Evolution of Oceanic Lithosphere: Kluwer, pp. 209-229.

LeBlanc M., Ceuleneer G., Al Azri H., Jedwab J., 1991, Concentration Hydrothermale de Palladium et Platine dans les Peridotites Mantellaires du Complex Ophiolitique: C. R. Acad. Sci. Paris, pp. 1007-1012.

Lorand, J. P., & Juteau, T., 2000, The Haymilyah Sulphide Ores (Haylayn Massif, Oman Ophiolite): In Situ Segregation of PGE-poor Magmatic Sulphides in a Fossil Oceanic Magma Chamber: Marine Geophys. Res., V21, pp. 327-349.

Moreno T., Gibbons, W., Prichard, H. M., Lunar, R., 2001, Platiniferous Chromite and the Tectonic Setting of Ultramafic Rocks in Cabo Oretegal, NW Spain: J. Geol. Soc. Lond., V158, pp. 601-614.

Nehlig, P. & Juteau, T., 1988, Flow Porosities, permeabilities and preliminary data on fluid inclusions and fossil thermal gradients in the crustal sequence of the Sumail Ophiolite: Tectonophysics, V151, pp. 199-221

Page N. J., Pallister J.S., Brown M.A., Smewing, J.D., Haffty, J., 1982, Palladium, platinum, rhodium, ruthenium and iridium in chromite-rich rocks form the Semail ophiolite, Oman: Can. Mineral., V20, pp. 537-548.

Racey, A., 1994, Biostratigraphy and Palaeobiogeographic Significance of Tertiary Nummmulitids (foraminifera) from Northern Oman: in Simmons M.D. (ed.) "Micropalaeontology and Hydrocarbon Exploration in the Middle East", Brit. Micropal. Soc. Pub. Series., pp. 343-369.

Sassani and Shock , 1998, Solubility and Transport of Platinum group Elements in Supercrital Fluids: Summary of Estimates of Thermodynamic Properties of Ru, Rh, Pd, Pt solids, aqueous ions and complexes to 1000ºC and 5 Kb: Geochim. Cosmochim. Acta., V.62, pp.2643-2671

Stanger, G., 1984, The Hydrogeology of the Oman Mountains: PhD Thesis, Open University, UK, 355 pp.

Stanger, G., 1985, Silicified serpentinite in the Semail Nappe of Oman: Lithos, V18, pp13-22.

Stanger, G., Neal, C., 1984, Calcium and Magnesium Oxide Precipitation from Alkaline Groundwaters and their Significance in the Process of Serpentinization: Min. Mag., V48/2, pp. 237 – 241.

Villey M., Le Metour, J. and De Gramont, X., 1986, Geological Map of Fanjah, Sheet NF40-3F. Explanatory Notes, BRGM & Oman Ministry of Petroleum & Minerals, 67 pp.

Worthing M.A. and Wilde A.R., 2002, Petrology, Geochronology and Tectonic Setting of Basanites from Eastern Oman: J. Geol. Soc. Lond., 159, pp. 469-483

Ziegler U., Stoessel F., and Peters, T., 1991, Meta-Carbonatites in the Metamorphic Series Below the Semail Ophiolite in the Dibba Zone, Northern Oman Mountains: in Peters T. (ed), "Ophiolite Genesis and Evolution of the Oceanic Lithosphere", Ministry of Petroleum and Minerals, Sultanate of Oman, pp. 627 – 645.